12-19-1999

The Kuroshio Region off Southwest Japan ASUKA 1993-95 Inverted Echo Sounder Data Report

Jeff Book

Karen L. Tracey
University of Rhode Island, krltracey@uri.edu

Mark Wimbush
mwimbush@uri.edu

Hiroshi Ichikawa

Shiro Imawaki

See next page for additional authors

GRADUATE SCHOOL OF OCEANOGRAPHY
UNIVERSITY OF RHODE ISLAND
NARRAGANSETT, RHODE ISLAND 02882–1197

The Kuroshio Region off Southwest Japan ASUKA 1993–95 Inverted Echo Sounder Data Report

GSO Technical Report No. 99-1

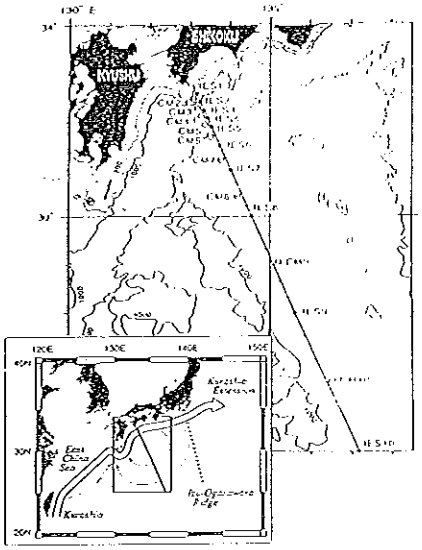

Jeff Book*
Karen L. Tracey
Mark Wimbush
Hiroshi Ichikawa†
Shiro Imawaki‡
Hiroshi Uchida‡§
Hideki Kinoshita¶

1999 December 19

*Present address: Naval Research Laboratory, Stennis Space Center, MS 39529
†Faculty of Fisheries, Kagoshima University, 4–50–20 Shimorata, Kagoshima 890–0056, Japan
‡Research Institute of Applied Mechanics, Kyushu University, Kasuga, Fukuoka 816–8580, Japan
§Present address: Japan Science and Technology Corporation, Kawaguchi, Saitama 332-0012, Japan
¶Ocean Surveys Division, Hydrographic Department, Maritime Safety Agency, 5-3-1 Tsukiji, Chuo-ku, Tokyo 104, Japan. Present address: Maritime Disaster Prevention Division, Maritime Safety Agency, 2-1-3 Kasumigaseki, Chiyoda-ku, Tokyo 100-8989, Japan

Contents

List of Figures

List of Tables

1 Introduction

In order to study the time-varying volume and heat transports of the Kuroshio off southwest Japan, a large number of scientists from Japan and a small number from the U.S.A. formed a group called ASUKA[1]. This group carried out a coordinated investigation which was concentrated in time on the years 1993–95, and in space on a 1,000 km segment of a TOPEX/POSEIDON suborbital track running south-southeast from western Shikoku.

This report describes the techniques used to process data collected by ten inverted echo sounders (IES) on this 1,000 km line off Japan, as part of the ASUKA study. The University of Rhode Island (URI) was responsible for all the IES's except IES5 and IES8 which were from the Hydrographic Department of the Japanese Maritime Safety Agency (MSA/HD). The URI IES's were deployed from the Training Vessel *Keiten-maru* in October 1993 and recovered from the same vessel in November 1995. The MSA/HD IES's were deployed from the Survey Vessel *Shoyo* in July 1993. IES8 was recovered by *Shoyo* in May 1994, but unfortunately IES5 was not recovered.

2 The ASUKA Study

The IES portion of the ASUKA study consisted of a line of ten IES's extending offshore from Cape Ashizuri on the island of Shikoku and oriented to lie along a track of the TOPEX/POSEIDON (T/P) satellite altimeter. The track chosen, oriented toward 155°True, is approximately perpendicular to the mean path of the Kuroshio through the ASUKA region (Figures 1 and 2). The spacings between IES instruments were chosen to provide high resolution sampling of the area where the Kuroshio would most likely cross the line and diminished resolution in the Kuroshio countercurrent. IES's 1–4 were moored at relatively shallow depths (< 2500 m) down the continental slope, while IES's 6–10 were moored in the Shikoku Basin at depths greater than 4000 m. Table 1 lists the locations and depths of the IES's.

The ASUKA Group deployed an array of nine current-meter moorings, designated CM2 through CM10 for the two-year period in which the URI IES's were gathering data. The positions of these moorings are shown in Figures 1 and 2. Table 2 lists the locations and depths of these current meters, but this report covers only the IES data and does not discuss the current-meter data.

Following recovery of the IES and current-meter arrays in November 1995, additional IES's (some pressure-gauge-equipped) have been maintained at sites IES1 and IES7. But this report covers only IES data from the 1993–95 deployment.

[1] Affiliated SUrveys of the Kuroshio off Ashizuri-misaki (i.e., Cape Ashizuri).

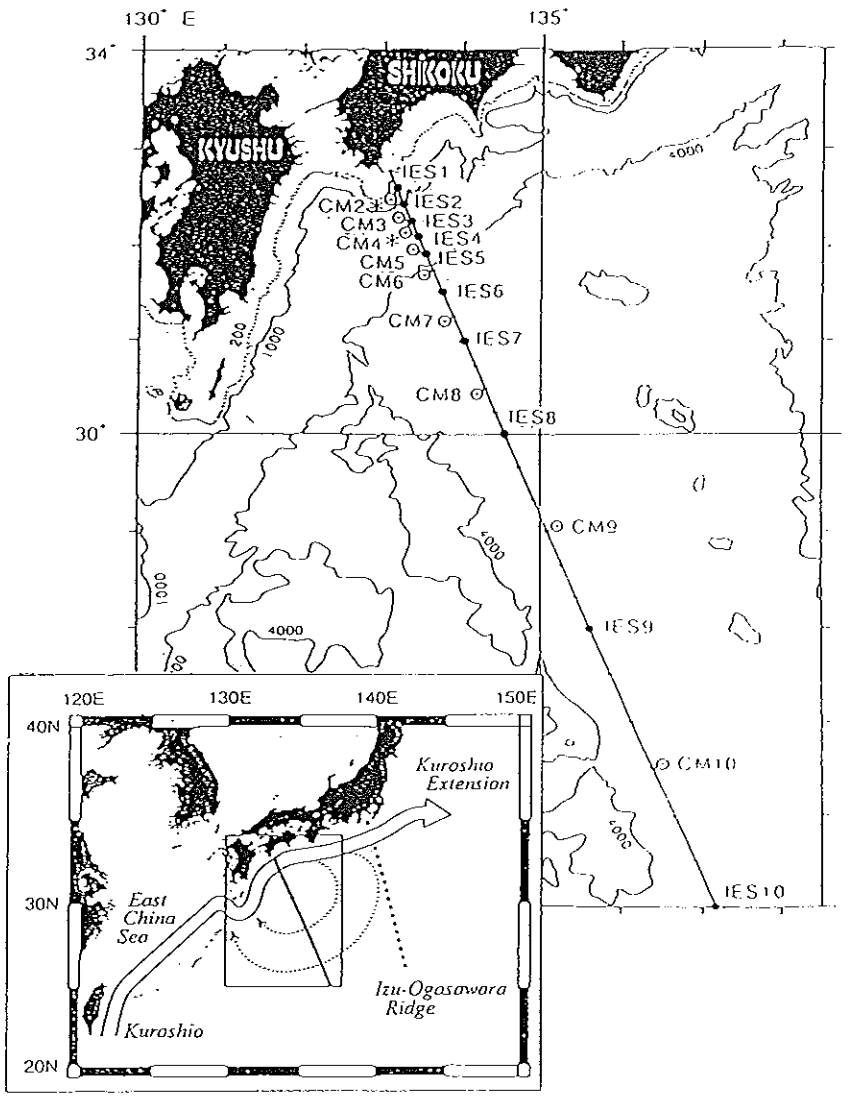

Figure 1: Geographic locations of principal ASUKA measurements. Solid circles (large or small) mark sites where hydrographic profiles were usually taken. The larger solid circles also indicate the sites of IES's. Bull's eyes are current-meter-mooring sites. Current-meter moorings with asterisks were topped by upward-looking ADCP's. Solid line indicates the main "ASUKA line." The T/P track is parallel to this line and lies approximately 8 km to the west-southwest. Lower panel shows a sketch of the mean Kuroshio path and recirculation in this region.

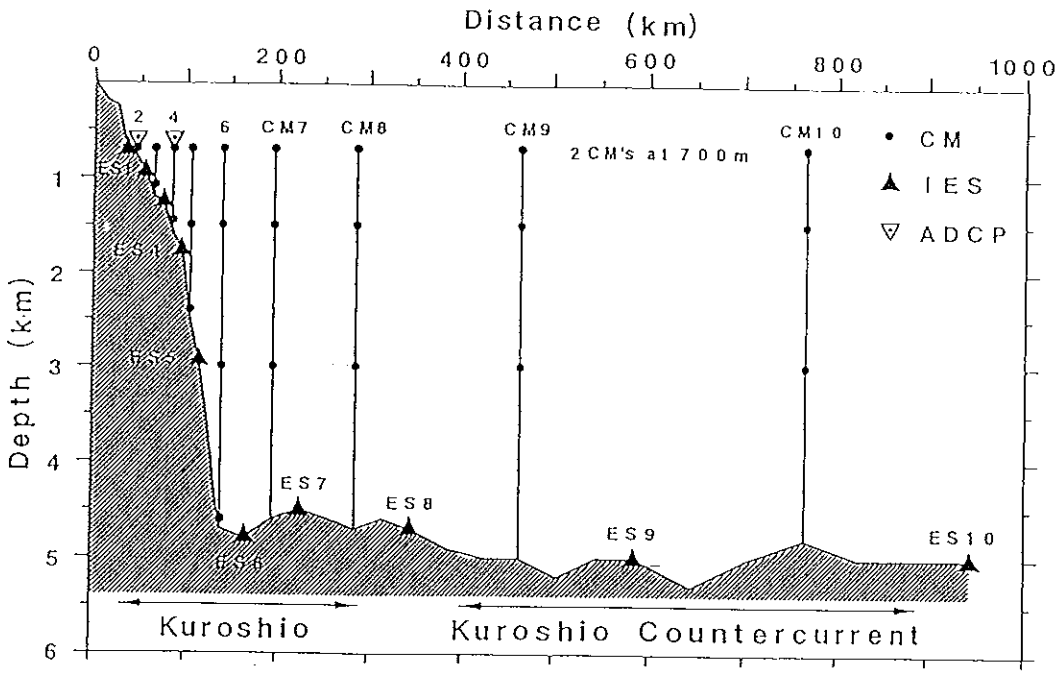

Figure 2: Cross section of the ASUKA line. Current-meter moorings are shown as solid lines with dots indicating the nominal depth of each current meter. IES's are indicated by triangles (IES1–IES10 are labelled ES1–ES10 in this figure only) and were located on the bottom (shaded region). IES depths shown are approximate; more accurate values are given in Table 1. IES5 was not recovered.

Instrument	Responsible Institution	Instrument Serial No.	Latitude	Longitude	Offshore Distance (km)	Spacing (km)	Depth (m)
IES1	URI	82	32.5865°N	133.2044°E	22.16		830
IES2	URI	83	32.4165°N	133.3011°E	43.12	— 20.96 —	960
IES3	URI	84	32.2506°N	133.3848°E	63.17	— 20.05 —	1190
IES4	URI	87	32.0836°N	133.4820°E	83.86	— 20.69 —	2020
IES6	URI	86	31.5019°N	133.7990°E	155.15	— 71.29 —	4880
IES7	URI	85	31.0046°N	134.0651°E	215.96	— 60.81 —	4450
IES8	MSA/HD	103	30.0017°N	134.5983°E	338.62	—122.66—	4630
IES9	URI	77	27.9967°N	135.6179°E	582.63	—244.01—	5270
IES10	URI	88	25.0033°N	137.0534°E	944.84	—362.21—	5050

Table 1: Locations and depths of IES instruments on the ASUKA line. Offshore distance is measured from Cape Ashizuri (32.733°N, 133.017°E) along the ASUKA line oriented toward 155°True. Spacing is the distance between instruments measured along that line. The depths are given to the nearest 10 m. (Note: Locations given are GPS ship positions at the time of IES deployment; IES on-bottom positions are unkown but are presumably within 1 km of these locations.)

The data in this report principally cover a two year period between 1994 yeardays[2] –66 and 686. Data were obtained from all URI IES's for this period. The data from IES8 extend between 1994 yeardays –176 and 131. These two time intervals overlap for almost 200 days.

3 Measurement

An IES measures the round-trip travel time of an acoustic pulse from the sea floor, where the IES is moored, to the sea surface (Chaplin and Watts 1984). The IES's used in this study were manufactured by URI. Every hour, they emitted a group of twenty-four 10 kHz "pings" at 10-second intervals, and recorded the individual echo times. IES1, moored at 830 m, had an unusually large proportion of early echo returns with a tendency to occur at certain preferred echo times (Figure 3). This was perhaps caused by reflections from sea-floor features, made possible by the downward bending of acoustic rays at depths above the center of the sound channel.

[2]1994 yearday 0 is taken to be at 1994 January 1 00:00 GMT.

Instrument	Average Latitude	Average Longitude	Offshore Distance (km)	1st Deployment Pressure (dbar)	2nd Deployment Pressure (dbar)
CM021	32.47°N	133.17°E	33	693	686
CM031	32.30°N	133.27°E	55	620	634
CM033				1040	1059
CM041	32.14°N	133.36°E	73	619	687
CM043				1424	1488
CM051	31.96°N	133.46°E	96	695	595
CM053				1510	1403
CM054				2404	2288
CM061	31.69°N	133.62°E	128	687	575
CM063				1507	1391
CM064				3002	–
CM065				4596	4532
CM071	31.24°N	133.85°E	183	574	527
CM073				1392	–
CM081	30.47°N	134.26°E	279	520	–
CM083				1347	–
CM084				2849	–
CM091	29.04°N	135.18°E	460	493	656
CM093				1323	1485
CM094				2830	2989
CM101	26.53°N	136.43°E	764	457	766
CM103				1294	1596
CM104				–	3100

Table 2: Locations of ASUKA current-meter moorings and depths of current meters on these moorings. Offshore distance is measured from Cape Ashizuri (32.733°N 133.017°E) along the ASUKA line oriented toward 155°True. Most moorings were redeployed once during the two-year measurement time. Latitudes, longitudes, and distances are averages for these two deployments. Pressures are mean values for each deployment based on measurements with an internal gauge or on mooring-drag computations. Individual deployments may be up to 1.6 km from the given offshore distance. "–" indicates current-meter data for the mooring are unavailable during that deployment.

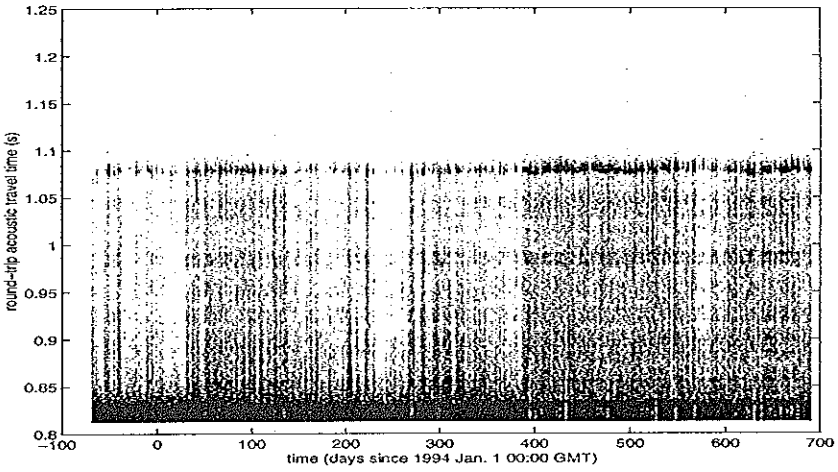

Figure 3: Entire set of echo returns from IES1 before processing. The echo returns with travel times close to 1.075 s are the sea-surface echoes.

4 Processing

The processing generally followed the procedures described in Fields et al. (1991). But our procedure differed in the low-pass filtering (see footnote below) and in the removal of seasonal signals (see Appendix D). Each set of 24 echo times recorded by the IES was analyzed to eliminate spurious echoes and form one representative echo time (τ) from the remainder. The τ data were despiked and then low-pass filtered[3] with a 48-hour cut-off period and subsampled at daily intervals. Example plots for IES data at each of these processing steps are shown as Figure 1 in Fields et al. (1991).

5 Data

Only variation about the mean in each τ was used for analysis, because the IES's lacked pressure sensors and therefore their depth could not be determined to the required accuracy. The time series for all nine IES's are shown in Figure 4. Hydrographic measurements from the ASUKA region are needed to interpret these τ data. A procedure is described in the Appendix to determine time series of vertical profiles for temperature and specific-volume anomaly from the IES data. Further details are given in Book (1998).

[3]using a 2nd order low-pass Butterworth filter applied twice, once forwards and once backwards, to eliminate phase error.

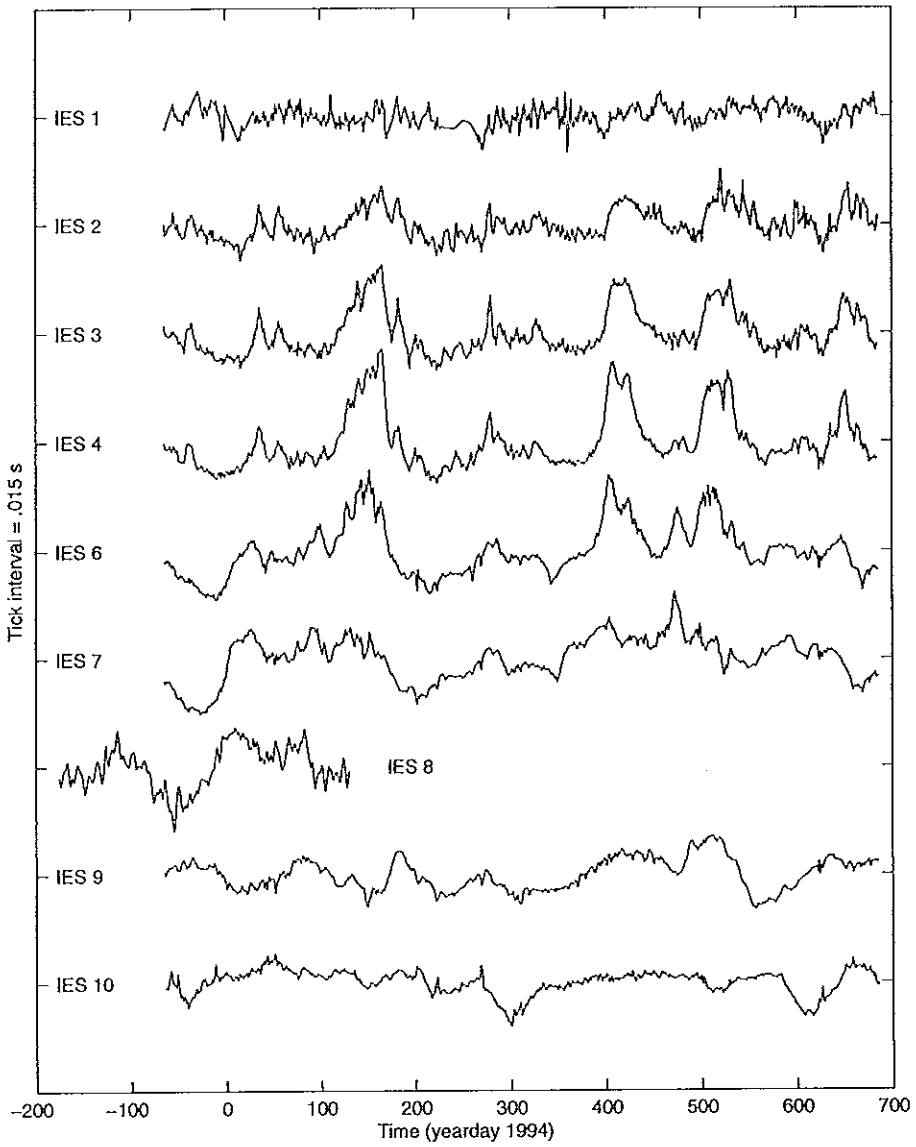

Figure 4: Time series of τ (without removal of seasonal signals) from the ASUKA IES's. Tick-marks on vertical axis are at time-series means, while their interval represents 0.015 s.

6 CD-ROM Disk

A CD-ROM is attached to the inside back cover of this report. It contains the echo times (τ) measured by the IES's, together with other files holding data useful in interpreting the τ time series.

The following text is taken from the highest-level "READ.ME" file on the CD-ROM.

> This disk, named ASUKAIES, contains the data discussed in GSO Technical Report No. 99–1, "The Kuroshio off Southwest Japan, ASUKA 1993–95 Inverted Echo Sounder Data Report." The data on this disk were prepared by Jeff Book.
>
> The disk is written in ISO 9660 format. It contains one hundred copies of the data. Even if some part of the disk becomes damaged, this may allow full data recovery. All copies are identical. Each one is in a directory named ASUKAI##, where ## is a two-digit number ranging from 00 to 99.
>
> Each ASUKAI## directory has four subdirectories. The main data are located in the TIMESERS subdirectory. These data are the processed inverted echo sounder (IES) acoustic echo time (τ) data discussed in Section 5 of the report and shown in Figure 4. This subdirectory also contains the IES location data shown in Table 1 of the report. The other subdirectories contain data which can be used as tools for the interpretation of the IES data. The CONVRSNS subdirectory contains data needed to convert the τ data in the TIMESERS directory to τ_{800} data (Equation 4). These files contain the information shown in Figures 16 and 18, discussed in Appendix F. The SLACTS subdirectory contains the SLACTS curves for τ, temperature, and specific-volume anomaly. The τ and temperature SLACTS curves are shown in Figures 11 and 12 respectively and are discussed in Appendix D. The GEMS subdirectory contains the GEM's and the error fields discussed in Appendices B, C, and E. These data are shown in Figures 6–9 of the report.
>
> The GEM's, SLACTS curves, and τ reference level conversions are only applicable for the ASUKA region. Moreover, the hydrographic means are only applicable to the 1993–95 ASUKA IES deployment time period.
>
> Summary of disk files:
>
> ASUKAI## directory
>
> READ.ME – this file
>
> TIMESERS subdirectory
>
> READ.ME – describes files in the subdirectory
> IESTS.DAT – IES time series
> IESLOC.DAT – IES positions and depths

CONVRSNS subdirectory

READ.ME – describes files in the subdirectory
TAUP800.DAT – coefficients to convert various τ references to τ_{800}
HYDRMEAN.DAT – mean values for hydrographic casts near each IES site

SLACTS subdirectory

READ.ME – describes files in the subdirectory
TAUSLAC.DAT – τ SLACTS curve
TEMPSLAC.DAT – temperature SLACTS curves
SVANSLAC.DAT – specific-volume-anomaly SLACTS curves

GEMS subdirectory

READ.ME – describes files in the subdirectory
TEMPGEM.DAT – temperature GEM
SVANGEM.DAT – specific-volume-anomaly GEM
TEMPGEME.DAT – error fields for the temperature GEM
SVANGEME.DAT – error fields for the specific-volume-anomaly GEM

7 Acknowledgements

The efforts of the captain (the late Prof. Yasutaka Yuwaki), crew and cadets of the *T/V Keiten-maru*, Faculty of Fisheries, Kagoshima University, were essential to the success of the URI IES deployment and recovery operations. Captain and crew of the *S/V Shoyo* were likewise helpful in the MSA/HD IES deployent and recovery operations. The repeated hydrography data on the ASUKA line were provided by members of the ASUKA Group, including M. Fukasawa, K. Hayashi, T. Hinata, H. Ichikawa, S. Imawaki, A. Kaneko, H. Kinoshita, K. Kutsuwada, K. Mimoto, A. Misumi, I. Nakano, K. Okuda, T. Saito, Y. Sekine, T. Shiga, T. Utsunomiya, H. Yoritaka and N. Yoshioka. Moored-current-meter data on the ASUKA line were provided by M. Fukasawa, H. Ichikawa and S. Imawaki. A part of the ASUKA study was supported by the International Cooperative Research Program of the Global Ocean Observing System (program leader: Keisuke Taira) sponsored by the Ministry of Education, Science, Sports and Culture, Japan.

D. Randolph Watts provided much useful advice and gave us access to many of the facilities and capabilities of his group. Michael Mulroney was repsonsible for the preparation, deployment and recovery of the URI IES's. The work of Mark Wimbush, Jeff Book and Karen Tracey was supported by the Office of Naval Research through grant N000149410023.

Appendix

A CTD/XBT Data

During the two-year ASUKA study, over 1000 hydrographic casts were taken in the region. These data were nearly equally divided between CTD and XBT casts. The processed hydrographic data used in this appendix were provided by the ASUKA Group. The hydrographic data underwent extensive quality-control checks. Salinity values for the XBT casts were inferred from the average temperature–salinity relationship of the CTD casts taken at the same location by the immediately preceding and immediately following hydrographic surveys. These data were used to interpret the τ data from the IES's.

B Gravest Empirical Mode (GEM)

A GEM represents the general structure of the current system as it varies with a vertically integrated quantity, such as acoustic echo time, τ. In the GEM method, the basic structure of the current system is reconstructed from hydrographic sections. τ is calculated for each cast in every section and then another variable such as temperature (T) or specific-volume anomaly (δ) is mapped as a function of measured pressure and calculated τ.

Figure 5 shows the distribution of T with τ and pressure for the ASUKA hydrographic sections. τ_{800} is τ referenced to a pressure level of 800 dbar. This pressure level is used as the common reference, because of the restricted number of hydrographic casts that extend deeper. The GEM is calculated by spline interpolation of these hydrographic data subsampled at 25 dbar intervals (starting at 25 dbar), and binned at 0.5 ms intervals. The data are interpolated and extrapolated in the horizontal using a cubic smoothing spline and then smoothed in the vertical using a fourth-order least-squares spline approximation. The parameters for the above splines were adapted from the ones used by Meinen (1998) and are briefly discussed in the next section.

The T GEM and the δ GEM are respectively shown in Figures 6 and 7. The GEM's shown in these figures have been seasonally corrected by processes described in sections D and E of this Appendix. Estimates of the error fields associated with the GEM's are calculated by comparing the original hydrographic measurements with the smoothed field. In each case the GEM is divided into bins with dimensions of 100 dbar by 3 milliseconds. The rms error for a bin is defined as the rms difference between the bin values and all the hydrographic measurements that fall within the bin (Figures 8 and 9, lower two panels). The percentage rms error for each bin is the rms error expressed as a percentage of range in the GEM at that pressure level (Figures 8 and 9, uppermost panel).

C Smoothing Parameters

The smoothing splines used by Meinen (1998) can be changed by adjusting a smoothing parameter or by changing a knot sequence. The smoothing parameter is associated with

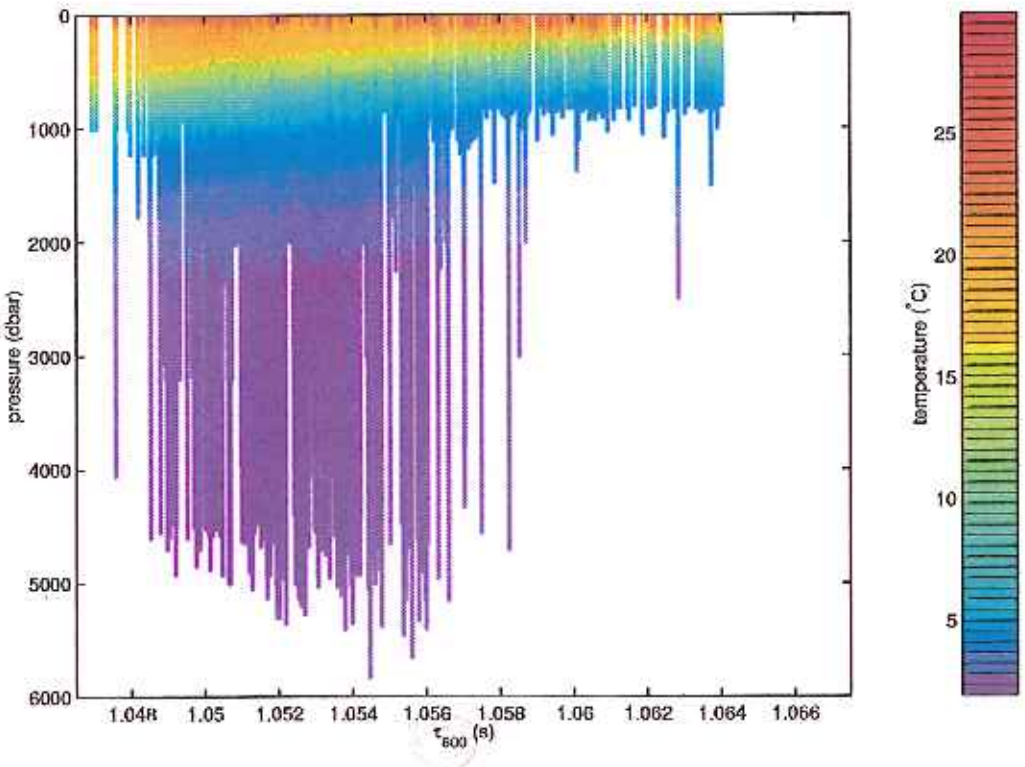

Figure 5: Distribution in τ_{800} and pressure of XBT/CTD data for the ASUKA study. The color of each point indicates the measured temperature. This data set is made up of 889 casts.

the cubic smoothing spline used to interpolate and extrapolate the data along a pressure level. The fourth-order least-squares spline approximation requires a knot sequence indicating pressure levels at which the spline is forced through the original value. These splines are described in more detail by de Boor (1992).

The smoothing parameter (p_s)[4] controls the flexibility of the spline. $p_s = 0.0$ forces the spline curve to take the shape of a straight line and allows no curvature, while $p_s = 1.0$ allows the spline to bend through every fitted point. A correct choice of this parameter allows the spline flexibility to model the perhaps complex curvature along a pressure level but enough stiffness to prevent rapid small-scale fluctuations. Based on qualitative visual judgment $p_s = 0.9999999$ was thought to fit the spline to the hydrographic data most satisfactorily.

At each knot for the vertical smoothing, the spline must pass through the value of the unsmoothed profile at that depth. The horizontal smoothing spline extrapolates for τ_{800} values not observed in the hydrography, producing near-linear changes in T and δ. If δ really

[4]called p in de Boor (1992).

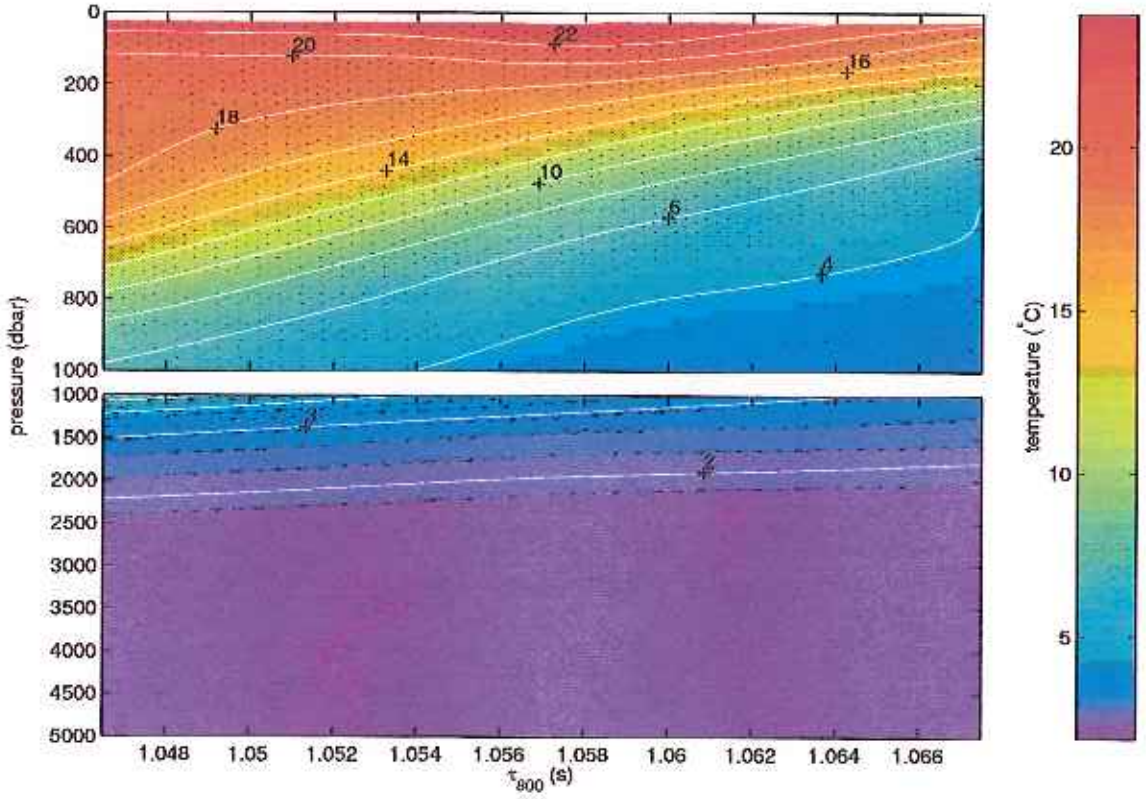

Figure 6: Temperature GEM for the ASUKA region. The blank region between the upper and lower panels indicates a change of scale. Contour intervals are 2°C (upper panel) and 1°C (lower panel). Seasonal corrections were applied to τ_{800} and iteratively to T in the top 150 dbar before smoothing to make this GEM (see Appendix sections D and E).

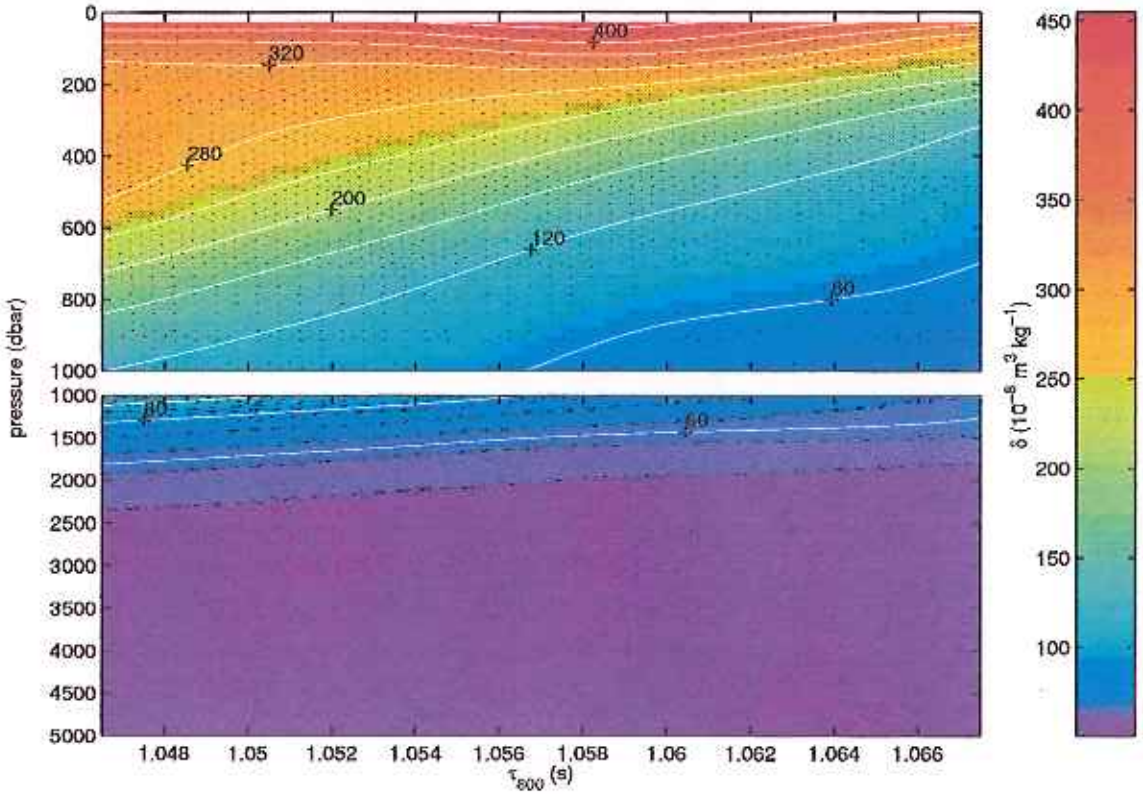

Figure 7: Specific-volume-anomaly GEM for the ASUKA region. The blank region between the upper and lower panels indicates a change of scale. Contour intervals are $40 \cdot 10^{-8}$ m^3/kg (upper panel) and $20 \cdot 10^{-8}$ m^3/kg (lower panel). Seasonal corrections were applied to τ_{800} and iteratively to δ in the top 150 dbar before smoothing to make this GEM (see Appendix sections D and E).

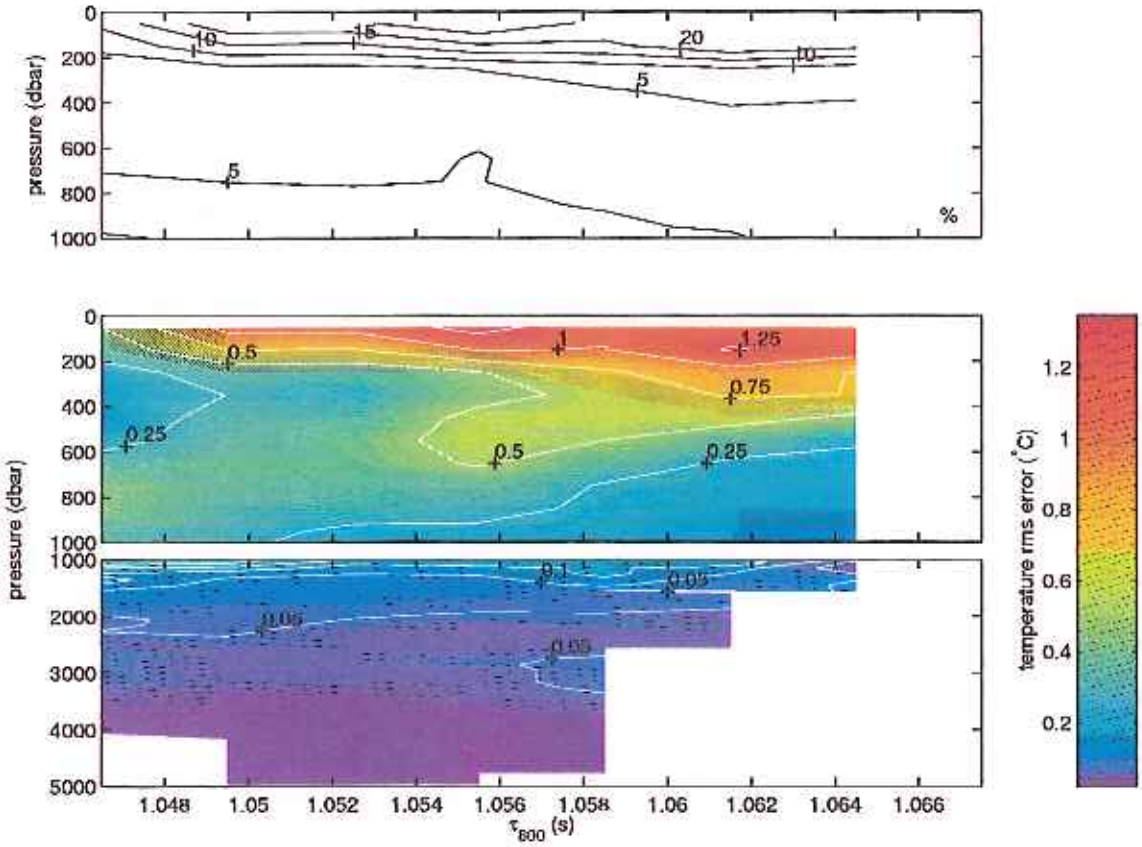

Figure 8: Error fields for the temperature GEM (Figure 6). The lower two panels are the rms error determined by subtracting the original hydrographic values from the smoothed field (see text). The uppermost panel is the percentage error calculated by dividing the rms error by the range in T that occurs at that pressure level, and multiplying by 100. The break between the lower two panels indicates a change of scale. Contour intervals are 5% (uppermost panel), 0.25°C (middle panel), and 0.05°C (lowermost panel). Blank areas indicate regions where no hydrographic data were available and extrapolation was used to calculate the GEM.

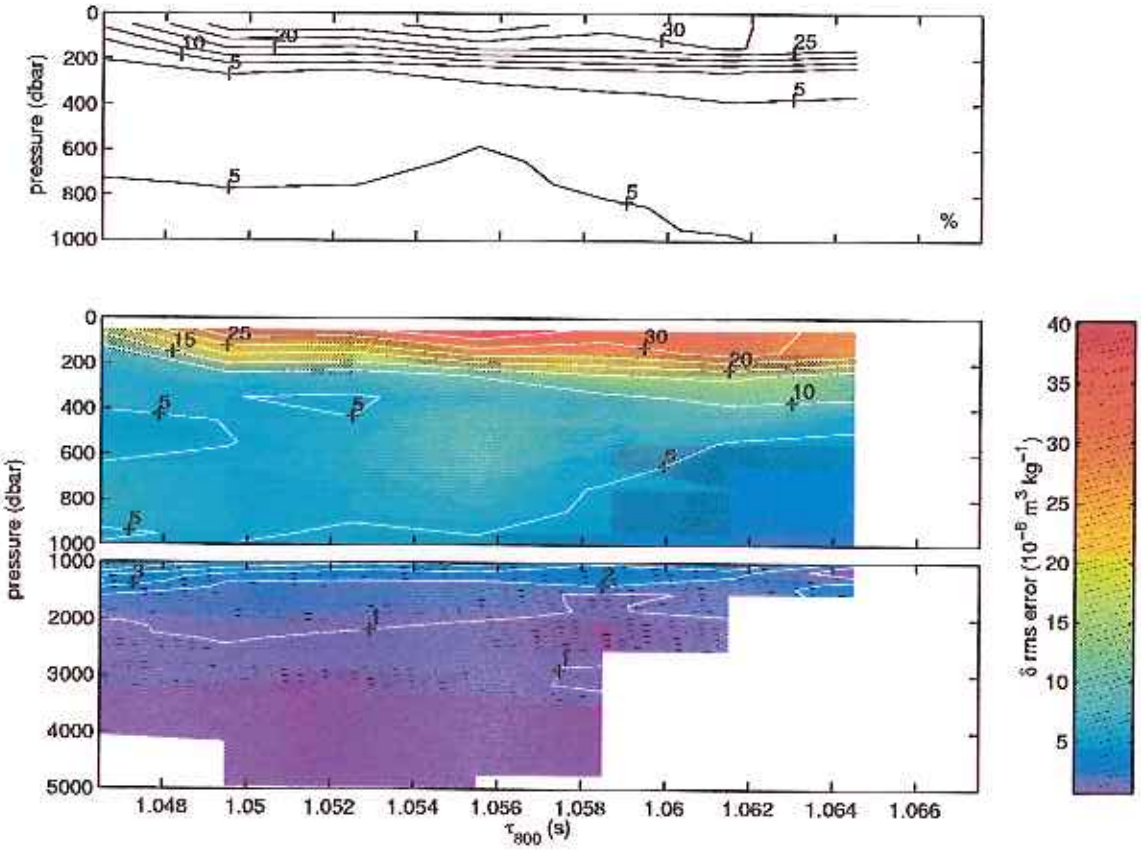

Figure 9: Error fields for the specific-volume-anomaly GEM (Figure 7). The lower two panels are the rms error determined by subtracting the original hydrographic values from the smoothed field (see text). The uppermost panel is the percentage error calculated by dividing the rms error by the range in δ that occurs at that pressure level, and multiplying by 100. The break between the lower two panels indicates a change of scale. Contour intervals are 5% (uppermost panel), $5 \cdot 10^{-8}$ m^3/kg (middle panel), and $1 \cdot 10^{-8}$ m^3/kg (lowermost panel). Blank areas indicate regions where no hydrographic data were available and extrapolation was used to calculate the GEM.

changed in such a nearly linear manner in the extrapolated region, then density inversions would occur at pressure levels around ~1100 dbar. The nonphysical linear changes produced by the smoothing spline extrapolation must be relaxed to eliminate density inversions in the upper water column. This was done by decreasing the total number of knots for the spline approximation and avoiding placing knots where T and δ were very non-linear. The knots used for the ASUKA region were at 25 and 50 dbar, at every 100 dbar in the range 100–1000 dbar, and at every 250 dbar in the range 1250–5000 dbar. Density inversions at ~1100 dbar are eliminated in the ASUKA δ GEM using this knot sequence.

The same parameters were used for both δ and T GEM's, although the values for these parameters were chosen based on the δ GEM. The overall structures present in both of these GEM's are similar and therefore new parameters do not need to be determined for the T GEM calculation.

D Seasonal Signals

In most regions of the ocean, there is a strong seasonal variation in the temperature-salinity characteristics of the surface layer. This Surface Layer Annual Cycle in Temperature and Salinity (SLACTS) signal should be removed before computing the GEM, so that seasonal bias in the data distribution does not affect the GEM calculation in the near-surface layers. The SLACTS signal can be identified in the hydrographic data as one-year-period oscillations, not necessarily sinusoidal, that are strongest in the surface mixed layer and decay with increasing depth. From the ASUKA CTD/XBT data, we identified and removed this signal from the IES data and the CTD/XBT data using a procedure described below.

Acoustic echo time is an integrated quantity, given by

$$\tau_P = 2 \times 10^4 \int_0^P \frac{dp}{\rho g c}, \tag{1}$$

where p is hydrostatic pressure, P is a reference-level pressure, ρ is density, g is acceleration due to gravity, and c is speed of sound. All units are standard SI, except for pressure which is in decibars.

As a first step in isolating and removing this surface-layer part of the seasonal signal in τ_P from the part associated with deeper disturbances, we computed a linear relationship between τ_P referenced to the bottom of the surface layer and τ_P referenced near the base of the main thermocline. We chose the bottom of the surface layer to be at a pressure level of 150 dbar, based on calculations made by James and Wimbush (1995). We use 1000 dbar as the reference level near the base of the thermocline because many hydrographic profiles do not extend below 1000 dbar. Any correlated signals appearing in both τ_{150} and τ_{1000} are presumably unrelated to large-scale seasonal changes in the surface layer due to local sea-surface fluxes. We computed a straight-line fit of τ_{150} to τ_{1000} and subtracted this linear trend from τ_{150} to form τ^*_{150}:

$$\tau^*_{150} = \tau_{150} - (\alpha \cdot \tau_{1000} + \beta), \tag{2}$$

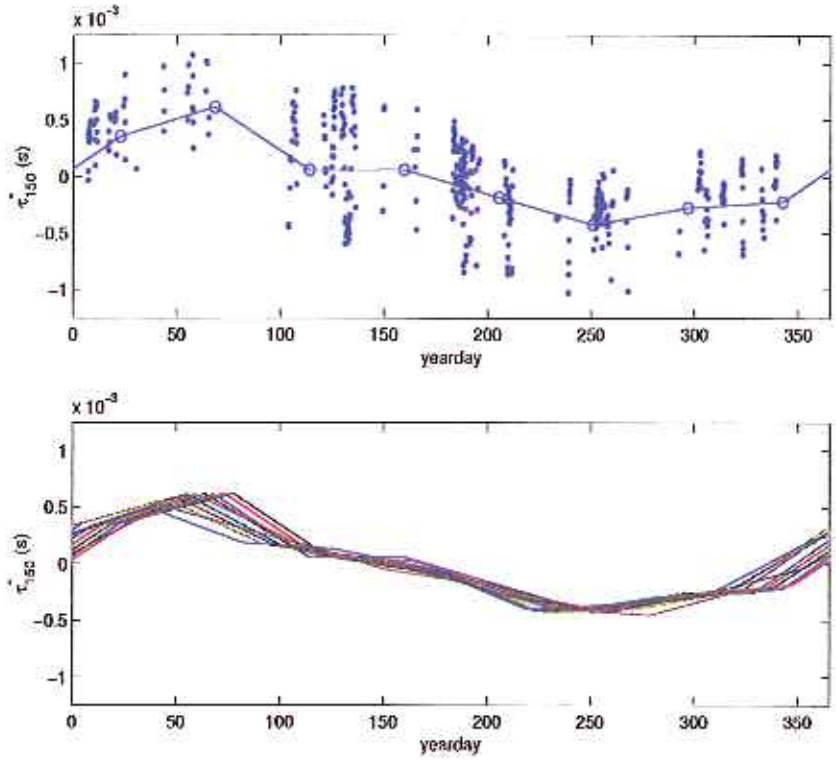

Figure 10: Steps in the procedure to find the τ SLACTS correction from τ^*_{150}. Upper panel shows the data (dots), the averaged data (circles), and the linear-interpolated curve (line) for an averaging with no shift. Lower panel shows all 10 linear-interpolated curves produced by interpolating averages shifted by 0, 10, 20, ... ,90% of the averaging bin width (1/8-year).

where α is the slope and β is the y-intercept.

The mean annual oscillation in τ^*_{150} is the SLACTS signal to be removed. We plotted τ^*_{150} according to the time of year that it was taken, so that a yearly signal could be computed. Averaging the data in eight 1/8-year bins and using linear interpolation produced a daily sampled curve from these averages (Figure 10, upper panel). By repeating this process each time, after shifting the centers of the bins in time by 10% of the bin length and wrapping the end of the year to the beginning, ten such daily sampled curves were produced (Figure 10, lower panel). The average of these ten curves is the final τ SLACTS curve, τ_s (Figure 11). This procedure reduces spurious effects due to the temporal irregularity of the CTD/XBT data, and produces a rather smooth curve whose end points match exactly. The SLACTS curve produced was subtracted from measured τ data, based on the yearday of the

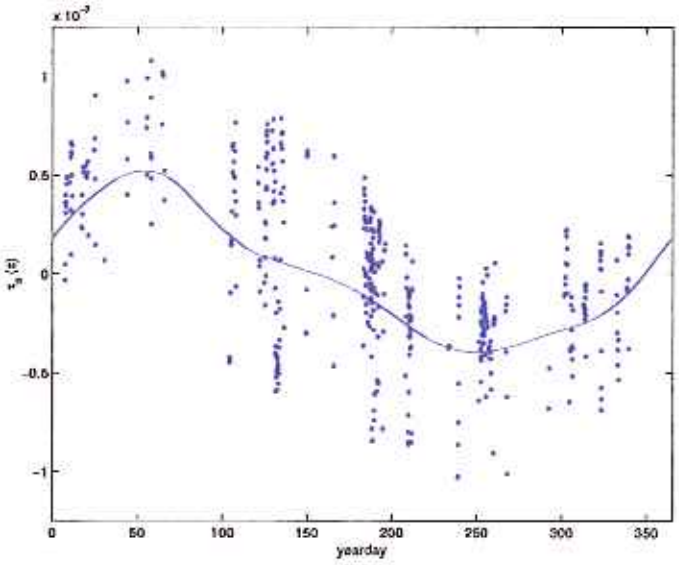

Figure 11: The SLACTS curve for τ_s, superimposed on the τ^*_{150} data from which it was computed. This curve is the average of the ten curves shown in the lower panel of Figure 10.

measurement, to produce a "SLACTS-corrected" value,

$$\tau_c = \tau_P - \tau_s \,. \tag{3}$$

To produce SLACTS curves for non-integrated variables, such as temperature or specific-volume anomaly, the interpolated-linear fit was done for each pressure level in the surface layer (see Appendix section E). This produced a set of SLACTS curves, each one associated with a different pressure level (Figure 12).

E GEM Iteration

There is a general trend in T across the Kuroshio that is the T GEM. If the spatio-temporal sampling is not uniform then the general GEM trend in the surface layer will interfere with the SLACTS signal calculation discussed in Appendix section B. Figure 13 shows that low τ_{800} measurements ($\tau_{800} < 1.051$ s), which predominantly occur far offshore (Figure 7), were not sampled during the winter months in the ASUKA hydrography.

Figure 14 shows various GEM's for the 25 dbar pressure level. The blue curve from this figure is the GEM calculated using SLACTS-corrected τ_{800} values but T data without a SLACTS correction applied. The T's are found to be high at low τ_{800} values. Some of

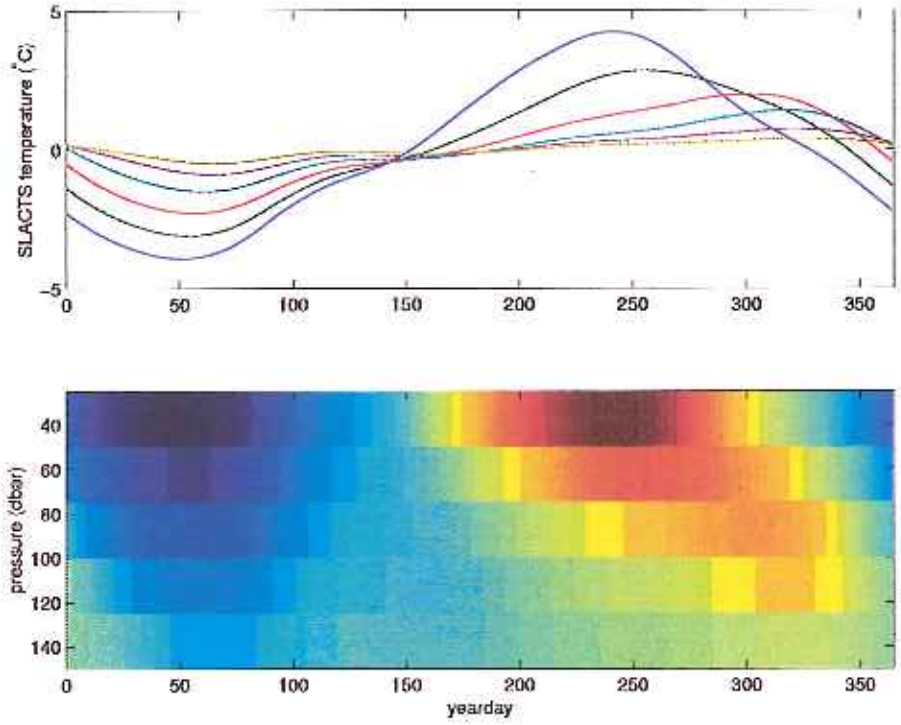

Figure 12: SLACTS curves representing the mean seasonal curves of T for various pressure levels in the surface layer. The upper panel shows the SLACTS curves for 25, 50, 75, 100, 125, and 150 dbar pressure levels. The amplitude of the SLACTS signal decreases with increasing depth. The lower panel shows the SLACTS signal as it is distributed in time and depth. Red indicates high T, blue indicates low T, and green indicates a SLACTS T signal near zero.

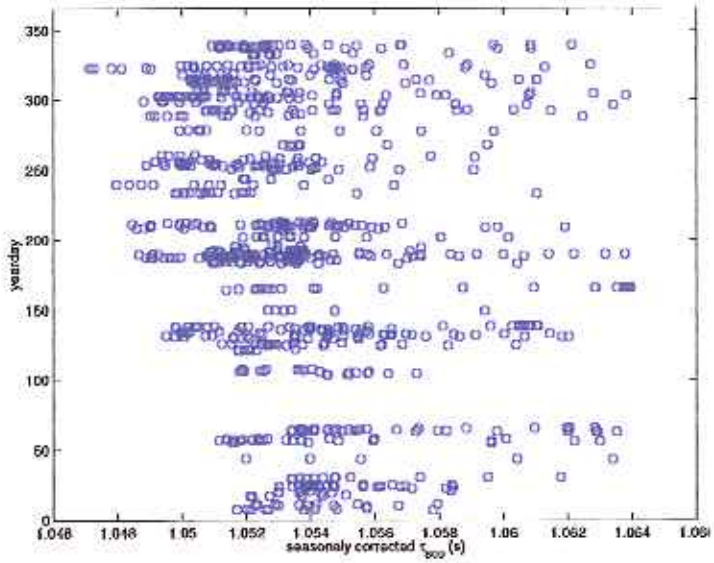

Figure 13: The seasonal distribution of τ_{800} measurements from the ASUKA hydrography. A seasonal correction has been applied to the τ_{800} data.

this trend is spurious because these low τ_{800} values were sampled during months when the surface layer tends to be warmer due to solar heating (Figure 12).

Clearly a SLACTS correction is needed for the T. A T SLACTS correction was computed from the T residual formed by subtracting the blue curve in Figure 14 from the raw 25 dbar data, and then performing a similar correction for T at the other levels down to 150 dbar. The sampling bias causes the T SLACTS curve for the warmer months to be too low, because much of the seasonal signal of the low τ_{800} region was incorporated into the GEM signal and therefore was not present as a residual. This T SLACTS correction was then subtracted from the original temperature data, the GEM was recomputed, and a new trend, the green curve, was found. The red curve in Figure 14 is the GEM calculated after applying an improved SLACTS correction derived from the residual of the raw T data and the green curve. The rms T error for the entire GEM was reduced from 0.6104°C to 0.4281°C to 0.4227°C by these three iterations (Figure 15, lower panel). Beyond the third GEM the errors do not significantly decrease and there is no convincing reason to continue iterating.

F Applying the GEM's to the IES data

The GEM provides a way of using measured τ data referenced to a specific pressure level to infer entire water column properties of oceanic variables. The τ measured by an IES

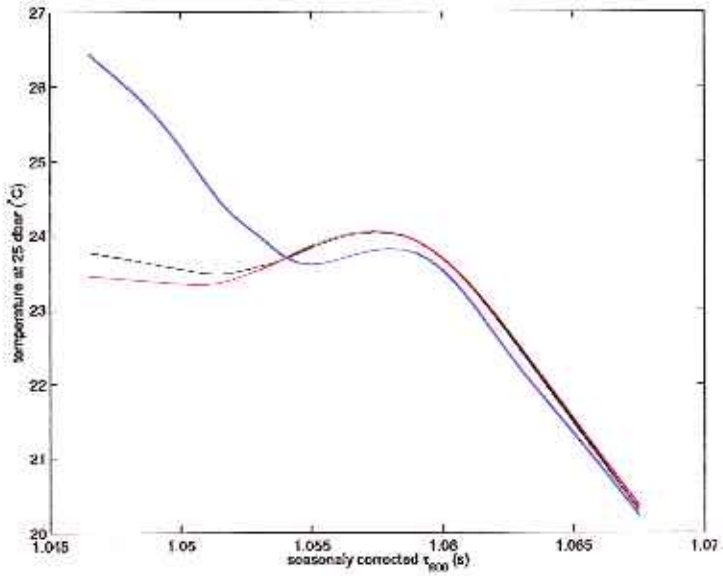

Figure 14: Various T GEM's calculated for the 25 dbar pressure level, where SLACTS effects are the largest. The τ_{800} data used for all the curves were SLACTS corrected. The blue curve used T data with no SLACTS correction, the green curve used T data with a SLACTS correction based on the residual of the data with the blue curve, and the red curve used T data with a SLACTS correction based on the residual of the data with the green curve. The red curve is used as the final GEM at this pressure level.

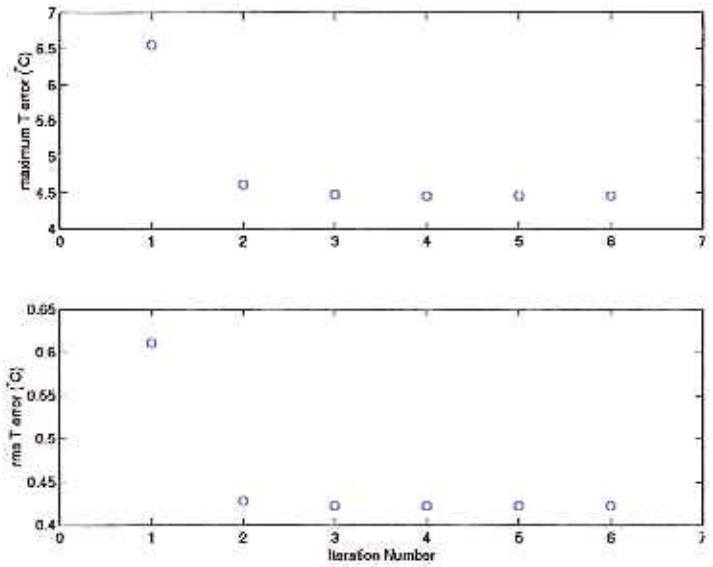

Figure 15: The errors associated with the T GEM iteration. The iteration number is the number of GEM fields that have been calculated. The maximum T error (upper panel) is defined as the value of the SLACTS-corrected T measurement with the largest absolute difference from the T GEM value for the same τ_{800} and pressure. The rms T error (lower panel) is defined as the rms of the SLACTS-corrected T measurements minus the corresponding T GEM values. All errors decrease as the number of iterations increases.

is referenced to the bottom[5], where the IES is moored, while the τ axis in the GEM is referenced to some other pressure level, where there are many hydrographic measurements. High correlations between τ's of different reference pressure levels allow conversion between pressure levels (Figure 16).

The slope (ψ) and y-intercept of the τ correlations could be used to convert the ${}^{IES}\tau_P$ data to τ_{800} data if the exact pressure level P of the IES were known, but only the approximate pressure level is known for each IES, and therefore only the variations, indicated by a prime, can be used with confidence. Multiplying ${}^{IES}\tau'_P$ by ψ produces a time series of ${}^{IES}\tau'_{800}$ at each IES site. The appropriate mean to be added to this time series can be determined from the mean of those hydrographic measurements that coincided in space and time with the IES deployments.

Figure 17 shows the locations in space, relative to the IES positions, of the hydrographic measurements taken during the ASUKA study. CTD/XBT casts within a 10 km radius of an IES, and occurring during that IES's operation time, were used to determine the mean τ_{800} to be used with the ${}^{IES}\tau'_{800}$ time series (Figure 18). This mean was added to ${}^{IES}\tau''_p$, defined as the fluctuations of ${}^{IES}\tau_p$ about the mean of ${}^{IES}\tau'_p$ sub-sampled at the CTD/XBT sampling times. The equation to convert an IES measurement to a τ_{800} measurement was thus

$$ {}^{IES}\tau_{800} = \psi \ {}^{IES}\tau''_P + \text{mean}({}^{CTD}\tau_{800}) \, . \tag{4} $$

The results of applying equation (4) to the IES data can be SLACTS-corrected (see Appendix sections D and E) and used with the GEM lookup maps to infer time series of δ and T profiles for each IES. Near the surface (0–150 dbar), the SLACTS curves for T or δ should be properly added back into the time series according to the yearday of each measurement. This will produce time series of vertical profiles of T and δ.

[5]more precisely about 1 m above the bottom.

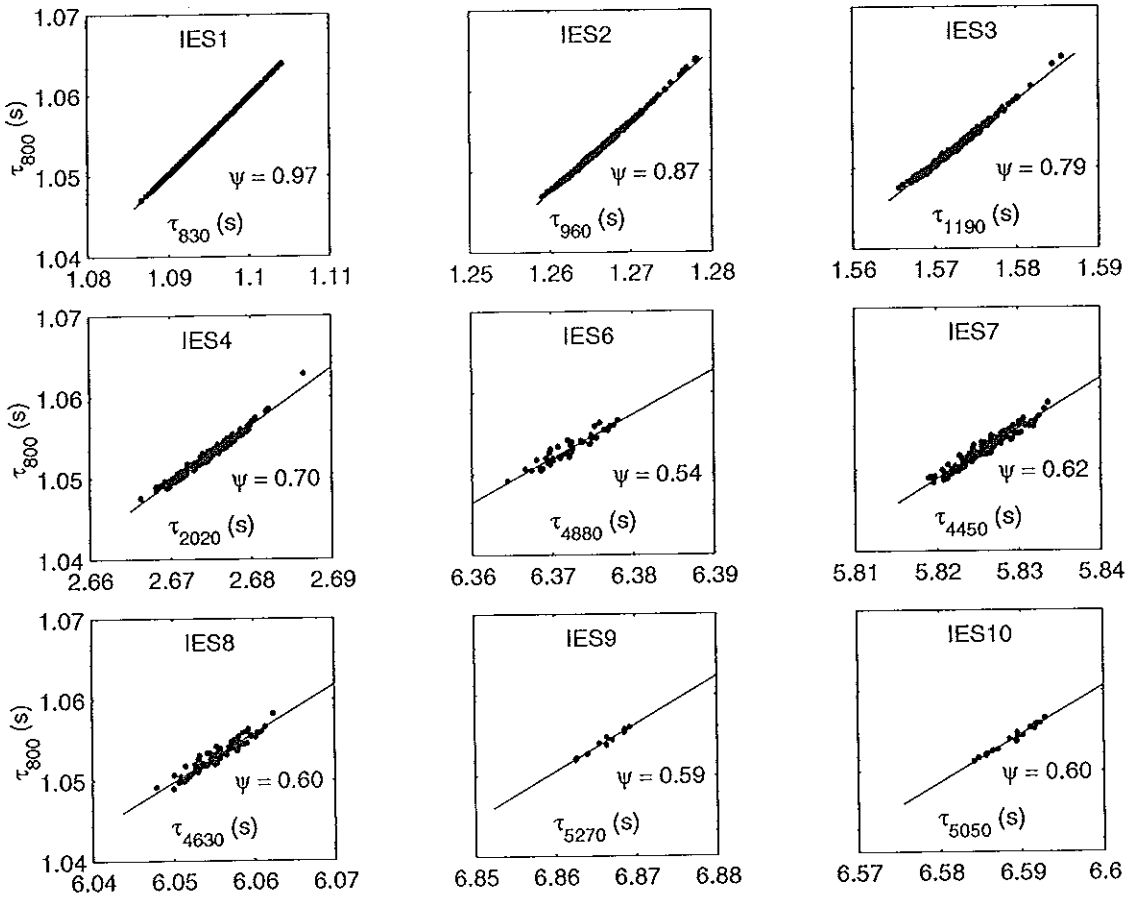

Figure 16: Correlations between τ_{800} and τ's referenced to the approximate pressure levels of the ASUKA IES instruments. All the correlation coefficients are above 0.91 at the 95% level of confidence. The slope of the least-squares fit line is indicated as the value of ψ in the lower right of each plot.

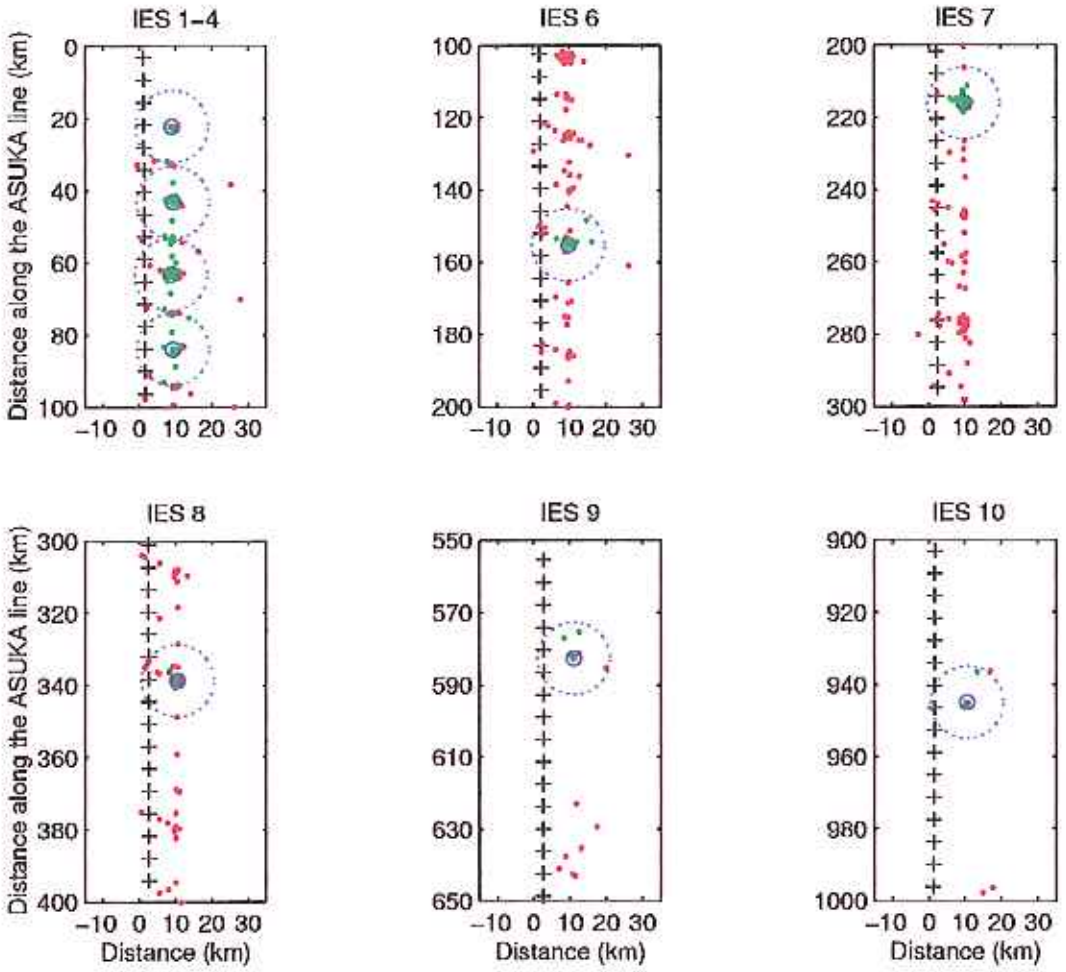

Figure 17: Locations of the IES's (centers of small blue circles), T/P measurements (black pluses), and hydrographic measurements (green and red dots) in the ASUKA study. Origin of the two distance axes is Cape Ashizuri. In each panel the vertical axis is distance along the ASUKA line (oriented toward 155°True) and the horizontal axis is oriented perpendicular to the ASUKA line (toward 65°True). Large dotted blue circles centered at the IES locations are at a radius of 10 km. All CTD/XBT measurements taken (a) inside these circles and (b) during the IES operation times, were used for IES data referencing (green dots). All other CTD/XBT casts were not used for this purpose (red dots).

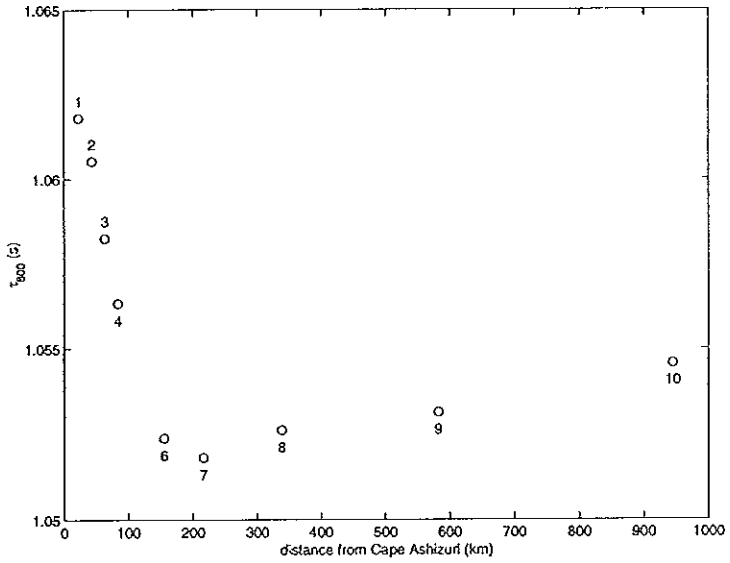

Figure 18: Mean τ_{800} for the sites of the IES's during the time of their data-gathering. The numbers refer to the IES's. The values of τ_{800} were computed from the hydrographic casts shown as green dots in Figure 17.

References

Book, J., 1998: Kuroshio variations off southwest Japan. Master's thesis, University of Rhode Island.

Chaplin, G. and D. R. Watts, 1984: Inverted echo sounder development. In *Proceedings of Oceans '84, IEEE-MTS Conference*, pp. 249–253.

de Boor, C., 1992: *Spline Toolbox User's Guide: for use with MATLAB.* The Math Works Inc.

Fields, E., K. Tracey, and D. R. Watts, 1991: Inverted echo sounder data processing report. Graduate School of Oceanography Technical Report 91-3, Graduate School of Oceanography, University of Rhode Island, Narragansett, RI 02882.

James, C. E. and M. Wimbush, 1995: Inferring dynamic height variations from acoustic travel time in the Pacific Ocean. *Journal of Oceanography*, **51**, 553–569.

Meinen, C. S., 1998: *Transport of the North Atlantic Current.* Ph. D. thesis, University of Rhode Island.